Journal of Sound and Vibration (1999) **228**(4), 923–930
Article No. jsvi.1999.2497, available online at http://www.idealibrary.com on IDEAL®

LINEAR DYNAMICS OF CURVED TENSIONED ELASTIC BEAMS

F. S. HOVER AND M. S. TRIANTAFYLLOU

Department of Ocean Engineering, Massachusetts Institute of Technology, 77 Massachusetts Avenue, Cambridge, MA 02139, *U.S.A.*

(*Received* 4 *November* 1998, *and in final form* 29 *June* 1999)

1. INTRODUCTION

Shallow-sag cables present a variety of unusual dynamic properties, caused by the coupling between transverse and axial vibrations provided by static curvature. Irvine's parameter λ [1] is central to the linear analysis:

$$\lambda^2 = \frac{EA}{\bar{T}}\left(\frac{wL}{\bar{T}}\right)^2, \tag{1}$$

where E represents Young's modulus, A the cross-sectional area of the cable, $\bar{T}$ the static tension in the cable (assumed constant along the length), w the cable's linear weight, and L its length. λ^2 is proportional to the ratio of elastic to catenary stiffness in the line, and through its mid-range, symmetric modes change shape and experience frequency crossover with respect to the non-changing antisymmetric modes.

The dynamics of arched and sagging beams with axial loading show a similarly rich behavior, again as a result of the curvature effects and extensibility [2–4]. In reference [5], Lu developed an asymptotic method to study the effects of bending stiffness on the canonical cable solution, reporting that the addition of bending stiffness moves the crossover points to higher values of λ and to higher frequencies. An important second parameter emerges that, with λ^2, governs the tensioned beam problem:

$$\Delta = \frac{EI}{\bar{T}L^2}, \tag{2}$$

where I is the sectional moment of inertia of the uniform beam. In this letter, we describe an alternative formulation to Lu's method [5], that results in explicit scalar equations, whose roots are the natural frequencies of the structure. We illustrate these modes and the associated dynamic tensions over a large range of bending stiffness.

2. DIFFERENTIAL EQUATIONS

We model the member as an elastic flexible rod under tension, and omit the effects of shear deformation and rotary inertia. The static configuration is assumed

0022-460X/99/490923 + 08 $30.00/0

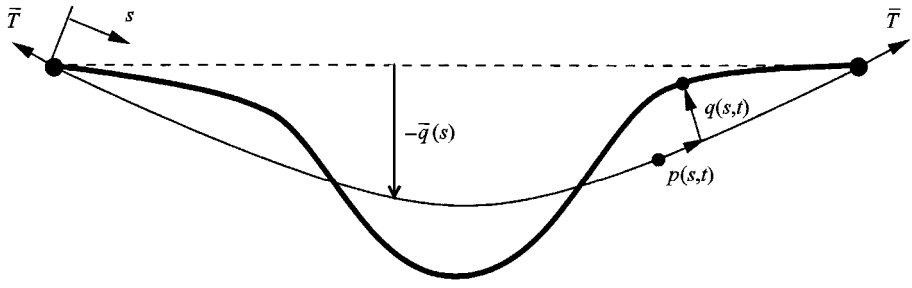

Figure 1. Deflection of the member from its static configuration given by the co-ordinates $p(s, t)$ (axial) and $q(s, t)$ (lateral).

to be contained within a vertical plane, and we consider here the in-plane dynamics only, as shown in Figure 1. Small lateral deflections $\bar{q}$ from the horizontal during static hanging are governed by the simplified beam equation

$$EI\frac{\mathrm{d}^4\bar{q}}{\mathrm{d}s^4} - \bar{T}\frac{\mathrm{d}^2\bar{q}}{\mathrm{d}s^2} + w = 0, \tag{3}$$

wherein if EI is small, the hanging cable with constant curvature $w/\bar{T}$ is recovered. As EI increases, the structure evolves from a horizontal catenary cable to a straight beam [6], and in the cases of one or both ends simply supported, the curvature becomes non-uniform along the length. In the case of clamped–clamped end constraints, with terminal angles matching the hanging cable (with no bending stiffness), variations in EI do not affect the shape at all. To keep the static configurations consistent for all values of bending stiffness, we deal only with this latter case.

Letting p and q denote the axial and lateral deflections respectively, and assuming a sinusoidal dependence on time such that $q = \tilde{q}\cos\omega t$, the equations of oscillating motion for a shallow-sag cable without bending stiffness are [7]

$$-m\omega^2\tilde{p} = EA(\tilde{p}'' - \alpha\tilde{q}'), \quad -m\omega^2\tilde{q} = \bar{T}\tilde{q}'' + \alpha EA(\tilde{p}' - \alpha\tilde{q}), \tag{4, 5}$$

where spatial derivatives are denoted by $'$, m is the linear mass of the cable, and $\alpha = w/\bar{T}$ is the static curvature. This form includes a dynamic tension component $\tilde{T}$ and a linear stress–strain relationship, such that $\tilde{T} = EA(\tilde{p}' - \alpha\tilde{q})$. We also have eliminated several terms from the listing in reference [7], using the assumptions $EA/\bar{T} \gg 1$ and $\tilde{q} \gg \tilde{p}$. Setting $\tilde{q} = \cos(ks)$, evaluation of the corresponding characteristic equation gives wavenumbers k and μ satisfying

$$k^2 = \frac{m\omega^2}{\bar{T}}, \quad \mu^2 = \frac{m\omega^2}{EA} - \alpha^2, \tag{6, 7}$$

where we have assumed further that $m\omega^2/EA > \alpha^2$, which is realistic in practical applications. We write the following mode shapes:

$$\tilde{p} = \frac{\alpha}{k}[c_1\sin ks - c_2\cos ks] + \mu[-c_3\sin\mu s + c_4\cos\mu s], \tag{8}$$

$$\tilde{q} = c_1\cos ks + c_2\sin ks + \alpha[c_3\cos\mu s + c_4\sin\mu s], \tag{9}$$

and these can be employed with the boundary conditions $\tilde{p}(\pm l) = \tilde{q}(\pm l) = 0$, where $l = L/2$, to obtain the natural frequencies and mode shapes found by Irvine and Caughey [1]:

$$\text{Antisymmetric: } \sin kl = 0, \tag{10}$$

$$p = -\frac{\cos \mu l}{\cos kl} \cos ks + \cos \mu s, \tag{11}$$

$$q = \frac{k \cos \mu l}{\alpha \cos kl} \sin ks + \frac{\alpha}{\mu} \sin \mu s; \tag{12}$$

$$\text{Symmetric: } \tan(kl) = kl\left(1 - \frac{4(kl)^2}{\lambda^2}\right), \tag{13}$$

$$p = -\frac{\alpha \cos \mu l}{k \cos kl} \sin ks - \frac{\mu}{\alpha} \sin \mu s, \tag{14}$$

$$q = \cos \mu s - \frac{\cos \mu l}{\cos kl} \cos ks. \tag{15}$$

The wavenumber k relates primarily to taut-string transverse deflections, while μ is a result of strong coupling between the axial and transverse motions.

The addition of bending stiffness to the above brings a new term $-EI\tilde{q}''''$ to the right-hand side of equation (5). The solutions thus derive from a sixth-order characteristic equation, and it can be shown with the assumptions so far that the approximate roots are: $\mu^2 = \pm(mw^2/EA - \alpha^2)$, and two other sets from the simplified case of zero curvature and inextensibility:

$$EI\tilde{q}'''' - \bar{T}\tilde{q}'' - m\omega^2\tilde{q} = 0. \tag{16}$$

One wavenumber pair corresponds to the sinusoidal mode $\tilde{q} = \cos(ks)$, and the other to the exponential $\tilde{q} = e^{\pm vs}$. The first we denote by k again, replacing the value of the previous section; the wave numbers and resulting mode shapes are

$$k^2 = \frac{-\bar{T} \pm \sqrt{\bar{T}^2 + 4m\omega^2 EI}}{2EI}, \quad v^2 = \frac{+\bar{T} \pm \sqrt{\bar{T}^2 + 4m\omega^2 EI}}{2EI}, \tag{17, 18}$$

$$\tilde{q} = c_1 \cos ks + c_2 \sin ks + c_3 e^{vs} + c_4 e^{-vs} + \alpha[c_5 \cos \mu s + c_6 \sin \mu s], \tag{19}$$

$$\tilde{p} = \frac{\alpha}{k}[c_1 \sin ks - c_2 \cos ks] + \frac{\alpha}{v}[c_3 e^{vs} - c_4 e^{-vs}] + \mu[-c_5 \sin \mu s + c_6 \cos \mu s]. \tag{20}$$

A frequency non-dimensionalization can be made from these results so far. Define

$$\tilde{\omega}^2 = m\omega^2 L^2/\bar{T} \tag{21}$$

to yield a parametrized version of (real) kl:

$$kl = \frac{1}{2}\sqrt{\frac{1}{2\Delta}[-1 + \sqrt{1 + 4\tilde{\omega}^2\Delta}]}. \tag{22}$$

For the nth taut-string mode, $kl = n\pi/2$, and equating this with the above gives an nth normalized frequency as $\tilde{\omega}_n = \sqrt{\Delta\pi^4 n^4 + \pi^2 n^2}$. As $\Delta \to 0$, $\tilde{\omega}_n \to n\pi$, recovering the taut-string case without stiffness. As $\Delta \to \infty$, $\tilde{\omega}_n \to \pi^2 n^2 \sqrt{\Delta}$, which is the correct value for simply supported pure bending. The normalization frequency ω_0 used in the plots of the next section is the dimensional form of $\tilde{\omega}_1$:

$$\omega_0 = \frac{1}{L}\sqrt{\frac{\bar{T}}{m}\left[\pi^4\Delta + \pi^2\right]}. \tag{23}$$

3. SOLUTION FOR CLAMPED–CLAMPED BOUNDARIES

The clamped–clamped boundary conditions are expressed in terms of the vibration amplitudes as follows: $\tilde{q}(\pm l) = 0$, $\tilde{q}'(\pm l) = 0$, and $\tilde{p}(\pm l) = 0$. These constraints with equations (19) and (20) lead to a 6×6 matrix $\mathbf{B}$ satisfying $\mathbf{Bc} = \mathbf{0}$, where $\mathbf{c} = \{c_1, c_2, c_3, c_4, c_5, c_6\}$. $\mathbf{B}$ can be reduced to a block-diagonal form $\tilde{\mathbf{B}}$ through a sequence of linear transformations, which preserve the determinant (see also reference [2]), and the condition $det(\tilde{\mathbf{B}}) = 0$ allows two separate equations, where the simplification $\sin \mu l \simeq \mu l$ follows from the assumptions:

$$\left[k\left(\frac{v^2}{\alpha^2} - 1\right)\cos kl \sinh vl + v\left(\frac{k^2}{\alpha^2} + 1\right)\sin kl \cosh vl\right]\mu^2 l + (k^2 + v^2)\sin kl \sinh vl = 0, \tag{24}$$

$$k\left(\frac{v^2}{\alpha^2} - 1\right)\sin kl \cosh vl - v\left(\frac{k^2}{\alpha^2} + 1\right)\cos kl \sinh vl + l(k^2 + v^2)\cos kl \cosh vl = 0. \tag{25}$$

The first of these has dependence on μ, while the second does not. Therefore, as in cables without bending stiffness, two fundamentally different types of modes exist: one involving primarily transverse motions of a taut string or beam, and another with strongly coupled axial and transverse motions.

Mode shapes for the structure are obtained by solving for $\mathbf{c}$. Setting $\tilde{c}_3 = 1$ and $\tilde{c}_6 = 1$, the 3×3 blocks in $\tilde{\mathbf{B}}$ give

$$\begin{bmatrix} \cos kl & \cosh vl \\ -k \sin kl & v \sinh vl \end{bmatrix}\begin{Bmatrix} \tilde{c}_1 \\ \tilde{c}_2 \end{Bmatrix} = \begin{Bmatrix} -\alpha \\ 0 \end{Bmatrix}, \tag{26}$$

$$\begin{bmatrix} \sin kl & \sinh vl \\ -\frac{\alpha}{k}\cos kl & \frac{\alpha}{v}\cosh vl \end{bmatrix}\begin{Bmatrix} \tilde{c}_4 \\ \tilde{c}_5 \end{Bmatrix} = \begin{Bmatrix} 0 \\ -\mu \end{Bmatrix}. \tag{27}$$

Employing the transformation back to $\mathbf{c}$ gives, for the first mode type (μ-dependent), the mode shapes

$$\tilde{p} = -\alpha^2\left[\frac{\mu^2}{\alpha^2}s + \frac{v^2 \sin ks \sinh vl + k^2 \sin kl \sinh vs}{kv(v \cos kl \sinh vl + k \sin kl \cosh vl)}\right], \tag{28}$$

$$\tilde{q} = \alpha\left[1 - \frac{v \cos ks \sinh vl + k \sin kl \cosh vs}{v \cos kl \sinh vl + k \sin kl \cosh vl}\right]. \tag{29}$$

For the second equation (μ-independent) we have

$$\tilde{p} = \frac{\alpha}{kv}\{k \sin kl\,[\cosh vl - \cosh vs] + v \sinh vl\,[\cos kl - \cos ks]\}, \tag{30}$$

$$\tilde{q} = \sin ks \sinh vl - \sin kl \sinh vs. \tag{31}$$

The frequency results are plotted in Figure 2, for the physical parameters $L = 100\,\text{m}$, $\bar{T} = 20\,\text{kN}$, $w = 10\,\text{N/m}$, and $EA = 200 \times 10^5\,\text{N}$; the remaining properties follow from equations (1) and (2). For low values of Δ, corresponding to very small bending stiffness, the results for cables are obtained, i.e., the kth symmetric and kth antisymmetric modes have coalescent natural frequencies (mode crossover) at values $\lambda/\pi = 2k$. The antisymmetric modes, independent of λ, show uniformly smooth transition from the cable values to the beam values. Symmetric modes, at small values of λ, also show smooth variation from cable to beam modes as Δ increases. For larger values of λ and in the mid-range of Δ, however, the symmetric-mode frequencies are substantially elevated, compared to a pure beam or cable with the same geometry. This effect diminishes progressively for higher-order modes, and the natural frequency of the kth symmetric mode is bounded above by the minimum value of the $(k + 1)$th symmetric mode at low λ.

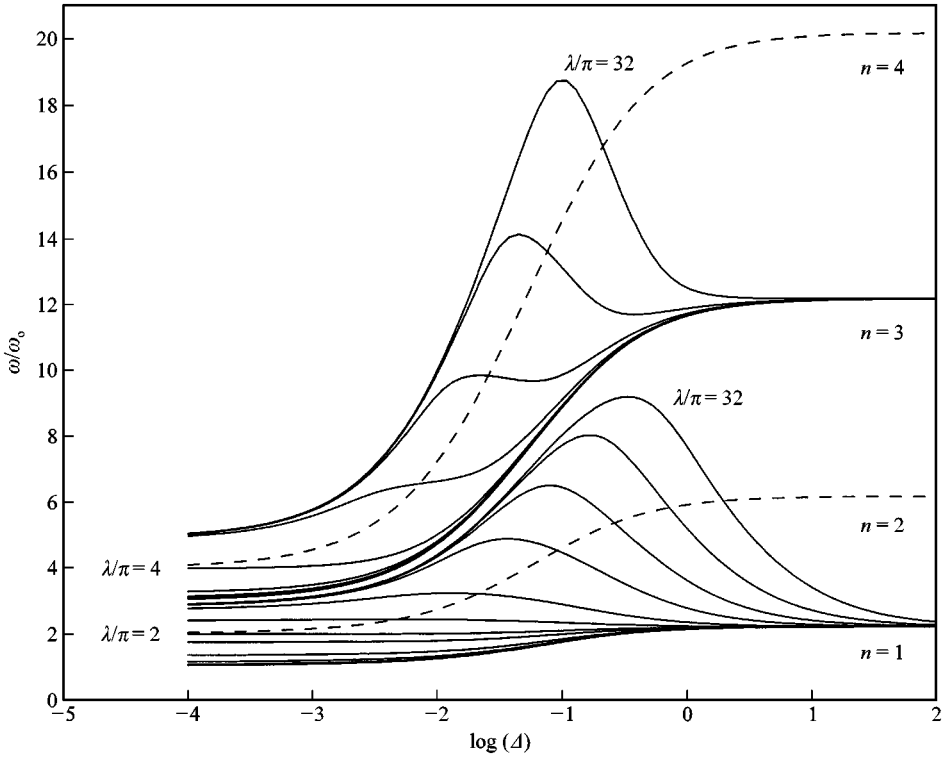

Figure 2. Normalized frequencies as functions of Δ and λ/π. Antisymmetric modes follow the dashed lines for all values of λ/π.

The elevated natural frequency of the symmetric modes for moderate Δ causes the crossover to occur at different values of λ, when compared to a pure cable, as Lu [5] found. For example, at $\log(\Delta) = -0{\cdot}7$, the crossover associated with the second antisymmetric mode occurs at $\lambda/\pi = 32$ instead of at 4. However, the behavior of the natural modes in the vicinity of a crossover point is qualitatively similar to that of a pure cable: along a curve of constant λ, moving from low towards high Δ the symmetric mode loses two lobes as it crosses an antisymmetric mode. Examples of mode shape transitions as functions of Δ are shown in Figure 3, for $\lambda = 32\pi$.

The peak dynamic tensions corresponding to the first two symmetric modes are plotted in Figures 4 and 5. The values shown are non-dimensionalized with the maximum deflection of $\tilde{q}$, and have the same overall scaling as used by Irvine and Griffin [8]. For the first mode, at values of λ/π above crossover, tensions grow significantly with bending stiffness, and are upper-bounded by the linear $\tilde{T} - \lambda/\pi$ relationship of the pure beam. The second mode of the pure beam also shows a linear trend, but with a reduced magnitude compared to the first mode. Further, at a given λ/π and as bending stiffness decreases, tensions increase to the level of the pure beam's first mode, and then decrease sharply. Thus, the first mode always has maximum tensions generated in the pure beam, but the second mode can reach maximum tension value at any intermediate bending stiffness, depending on λ/π. In all cases, the tension maxima are aligned with crossovers.

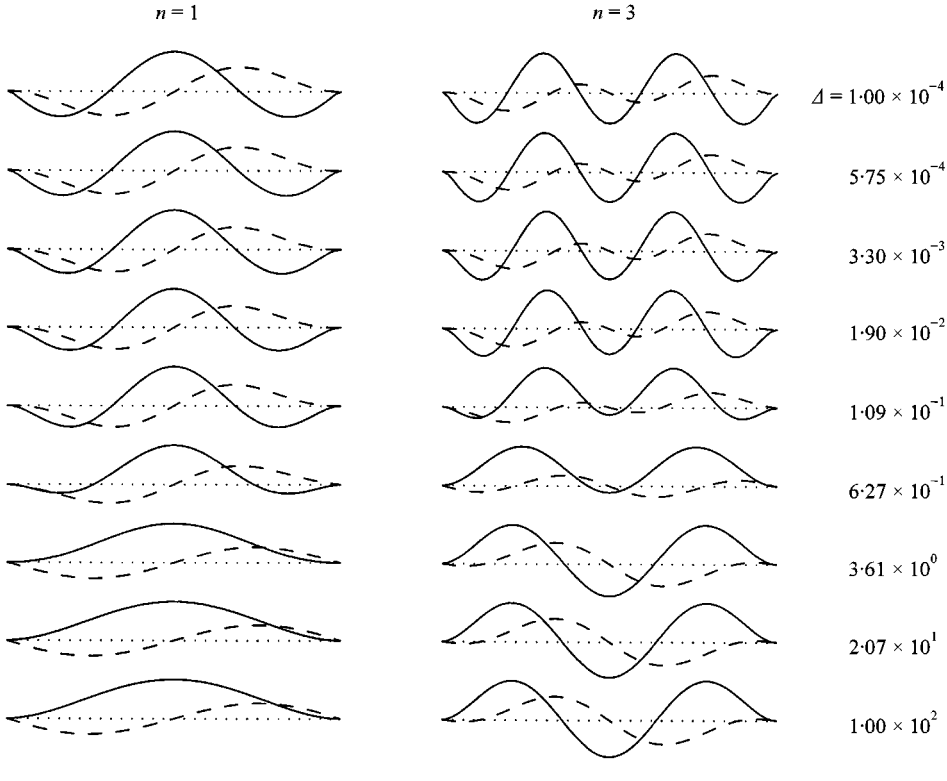

Figure 3. Symmetric modes, $\lambda/\pi = 32$. Dashed lines show $10 \times \tilde{p}(s)$, solid lines show $\tilde{q}(s)$.

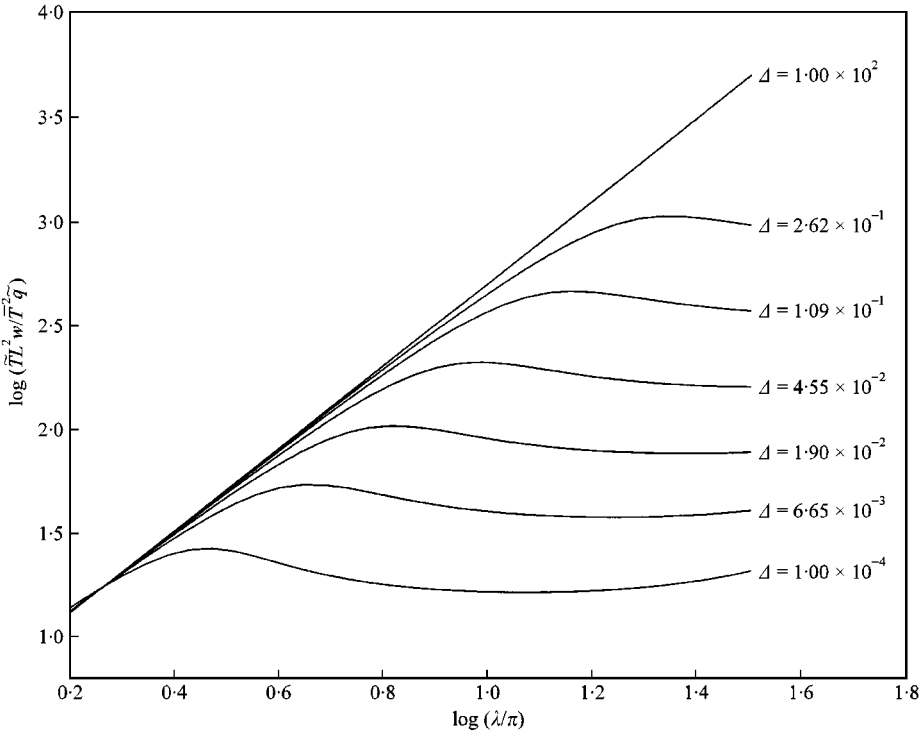

Figure 4. First symmetric mode dynamic tension.

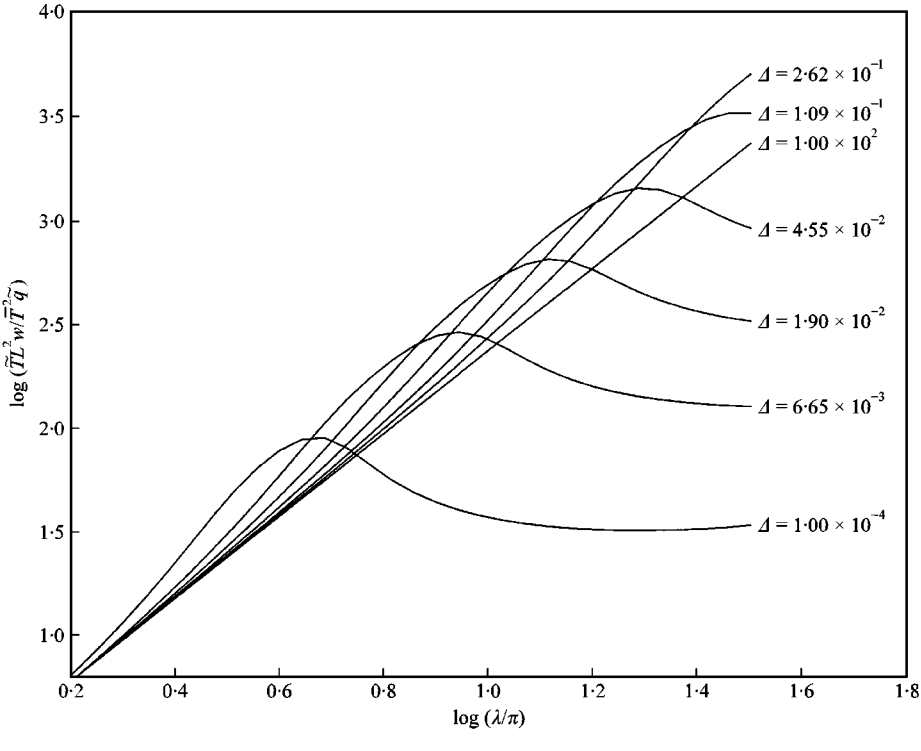

Figure 5. Second symmetric mode dynamic tension.

The significance of these findings pertains mainly to the amplification of modal frequencies, and to the variation of mode crossovers, which are accompanied by high dynamic tension. For the first two modes discussed, these properties are most sensitive in the range of Δ from 0·01 to 1.

ACKNOWLEDGMENT

This work was supported by the Office of Naval Research (Ocean Engineering Division), under Contract N00014-95-1-0106 and monitored by Dr. T. F. Swean, Jr.

REFERENCES

1. H. M. Irvine and T. K. Caughey 1974 *Proceedings of the Royal Society of London A* **341**, 299–315. The linear theory of free vibrations of a suspended cable.
2. A. S. Veletsos, W. J. Austin, C. A. Lopes Pereira, and S.-J. Wung 1972 *Proceedings of the ASCE, Journal of the Engineering Mechanics Division* **108**, 311–329. Free in-plane vibration of circular arches.
3. P. Chidamparam and A. W. Leissa 1993 *Applied Mechanics Reviews* **46**, 467–483. Vibrations of planar curved beams, rings, and arches.
4. P. Chidamparam and A. W. Leissa 1995 *Journal of Sound and Vibration* **183**, 779–795. Influence of centerline extensibility on the in-plane free vibrations of loaded circular arches.
5. C.-L. Lu 1994 *Doctoral Dissertation, University of Michigan.* Three-dimensional flexural and torsional mechanics of low and high tension cables.
6. J. Kevorkian and J. D. Cole 1985 *Perturbation Methods in Applied Mathematics.* New York: Springer-Verlag.
7. M. S. Triantafyllou 1984 *Quarterly Journal of Mechanics and Applied Mathematics* **37**, 421–440. The dynamics of taut inclined cables.
8. H. M. Irvine and J. H. Griffin 1976 *Earthquake Engineering and Structural Dynamics* **4**, 389–402. On the dynamic response of a suspended cable.